University of Montana

ScholarWorks at University of Montana

Biological Sciences Faculty Publications

Biological Sciences

10-23-2012

Scaling Flow Path Processes to Fluvial Landscapes: An Integrated Field and Model Assessment of Temperature and Dissolved Oxygen Dynamics in a River-Floodplain-Aquifer System

Ashley M. Helton

Geoffrey C. Poole

Robert A. Payn

Clemente Izurieta

Jack Arthur Stanford
The University of Montana, jack.stanford@umontana.edu

Follow this and additional works at: https://scholarworks.umt.edu/biosci_pubs

Part of the Biology Commons
Let us know how access to this document benefits you.

Recommended Citation

Scaling flow path processes to fluvial landscapes: An integrated field and model assessment of temperature and dissolved oxygen dynamics in a river-floodplain-aquifer system

Ashley M. Helton,[1,2] Geoffrey C. Poole,[3] Robert A. Payn,[3] Clemente Izurieta,[4] and Jack A. Stanford[5]

[1] Biogeochemical cycling within river ecosystems is strongly influenced by geomorphic and hydrologic dynamics. To scale point observations of temperature and dissolved oxygen (DO) to a hydrologically complex and dynamic three-dimensional river-floodplain-aquifer system, we integrated empirical models of temperature and biotic oxygen utilization with a recently published hydrogeomorphic model. The hydrogeomorphic model simulates channel flow, floodplain inundation, and surface-subsurface water exchange on the 16 km^2 Nyack Floodplain, Middle Fork Flathead River, Montana, USA. Model results were compared to observed data sets of DO to test the hypothesis that complexity in spatiotemporal patterns of biogeochemistry emerges from a comparatively simple representation of biogeochemical processes operating within a multidimensional hydrologic system. The model explained 58% of the variance in 820 DO measurements that spanned the study site longitudinally, laterally, vertically, and across river discharge conditions and seasons. We also used model results to illustrate spatial and temporal trends of temperature and DO dynamics within the shallow alluvial aquifer, which is an extensive hyporheic zone because subsurface alluvial flow paths are recharged primarily by channel water. Our results underscore the importance of geomorphic, hydrologic, and temperature dynamics in driving river ecosystem processes, and they demonstrate how a realistic representation of a river's physical template, combined with simple biogeochemical models, can explain complex patterns of solute availability.

1. Introduction

[2] Predictable one-dimensional patterns of solute concentrations occur along subsurface hydrologic flow paths at the scale of centimeters to meters as each solute is consumed and produced by biogeochemical processes [*Baker et al.*, 2000; *Hedin et al.*, 1998; *Vidon and Hill*, 2004, *Zarnetske et al.*, 2011]. As individual hydrologic flow paths diverge and converge within the surface and subsurface of larger river systems, different combinations of solutes are brought together, creating a three-dimensional landscape that encompasses a wide range of biogeochemical possibilities [*Fisher et al.*, 2004; *McClain et al.*, 2003]. Projecting our understanding of small-scale biogeochemical patterns to predict large-scale floodplain behavior requires a quantitative approach to integrating physico-chemical changes commonly observed along individual flow paths into complex hydrogeomorphic networks. Developing methods to scale observed one-dimensional biogeochemical patterns to three-dimensional river-floodplain-aquifer systems is fundamental for understanding the complex spatiotemporal patterns of biogeochemical cycling across fluvial landscapes.

[3] Rivers systems include hydrologically interdependent compartments: surface channel(s), the subsurface alluvial aquifer including the hyporheic zone, and the floodplain surface including riparian ponds, wetlands, and areas periodically inundated during high flow [*Stanford and Ward*, 1993]. Hydrologic flow drives the exchange of dissolved and particulate materials among river compartments, where

[1]Odum School of Ecology, University of Georgia, Athens, Georgia, USA.

[2]Now at Department of Biology, Duke University, Durham, North Carolina, USA.

[3]Department of Land Resources and Environmental Sciences, Montana State University, Bozeman, Montana, USA.

[4]Computer Science Department, Montana State University, Bozeman, Montana, USA.

[5]Flathead Lake Biological Station, Division of Biological Sciences, University of Montana, Polson, Montana, USA.

Corresponding author: A. M. Helton, Department of Biology, Duke University, Box 90338, Durham, NC 27708, USA. (amh72@duke.edu)
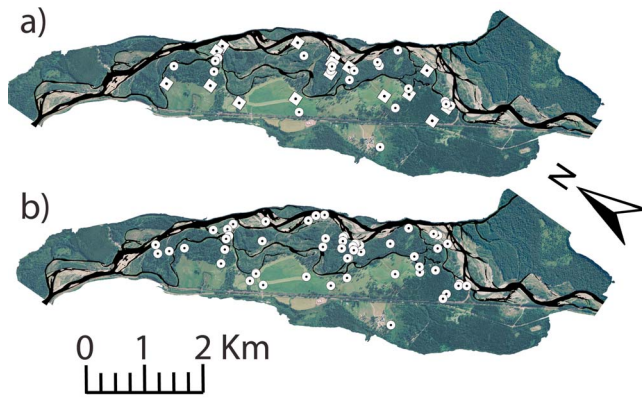
Figure 1. Aerial photo of the Nyack Floodplain of the Middle Fork Flathead River located in northwest Montana, USA (48°27′30″N, 113°50′W, 1010 m elevation) with (a) well locations with temperature records used for model parameterization (squares) and evaluation (circles) and (b) well locations with dissolved oxygen measurements used for model evaluation. River flows north.

these transported materials may be retained and transformed by various physical and biological processes [*Baker et al.*, 2000; *Dahm et al.*, 1998; *Fisher et al.*, 1998]. For example, when the ratio of subsurface to surface flow is high, microbial processes within hyporheic zones can account for the majority of whole ecosystem processes [*Fellows et al.*, 2001], and hyporheic water discharged back to the channel can influence surface water chemistry [*Dent et al.*, 2001] and temperature [*Arrigoni et al.*, 2008]. Thus, hydrologic dynamics of a river ecosystem control both the magnitude and rate of solute exchange among different river compartments, and the contact time between solutes and microbial communities within those compartments.

[4] Traditional methods that focus on understanding hydrologic connections between river compartments are inadequate for describing hydrologic fluxes at the fluvial landscape-scale (e.g., 10 s of meters to kilometers) and therefore the effects of hydrologic dynamics on biogeochemical fluxes and processes at the landscape scale [*Bencala et al.*, 2011]. Widely applied tracer techniques capture hydrologic exchanges that are short in time and space (hours to several days; centimeters to meters) [*Poole et al.*, 2008], and regional analysis of river gauges capture only the net (not the gross) hydrologic exchange between the river channel and other compartments over spatiotemporally coarser scales. Existing groundwater flow simulation models (e.g., MODFLOW) [*McDonald and Harbaugh*, 2003] are designed to simulate subsurface water movement and lack the ability to simulate dynamic patterns of inundation across complex, low-relief landscapes, like floodplains [*Jones et al.*, 2008]. Thus, such models lack the ability to describe spatiotemporal variability in surface water hydraulic head that drives hydrologic exchange [*Poole et al.*, 2006].

[5] Here, we used a recently published three-dimensional hydrogeomorphic model of a river-floodplain-aquifer system, the 16 km² Nyack Floodplain of the Middle Fork Flathead River [*Helton et al.*, 2012]. We linked the hydrogeomorphic model to empirical models of temperature and biotic oxygen utilization to simulate temperature and oxygen dynamics across the study site. The hydrogeomorphic model parameterization included analysis of a high resolution elevation data set to delineate geomorphic controls on inundation dynamics [*Jones et al.*, 2008] and thus represents detailed spatiotemporal variation in floodplain inundation, which drives additional hydrologic exchange between surface- and aquifer water.

[6] Our objective was to determine if a relatively simple, one-dimensional flow path biogeochemical model, when integrated within a sufficiently realistic three-dimensional hydrologic model, could explain complex spatial and temporal patterns in dissolved oxygen (DO) dynamics across the expansive shallow alluvial aquifer. Patterns in model output were compared to large observed data sets in both space (longitudinal, lateral, and vertical patterns within the floodplain) and time (across discharge conditions and seasonal variability) to determine whether spatiotemporal complexity in observed DO and temperature dynamics emerges from simple biogeochemical dynamics operating within the relatively complex hydrologic system of this Rocky Mountain alluvial river.

2. Study Site

[7] The study site is a 16 km² montane floodplain (Figure 1) on the gravel- and cobble-bedded Middle Fork of the Flathead River, located in northwest Montana, USA. The river is unregulated and most of the 2300 km² upstream catchment is in federally protected wilderness or Glacier National Park, including the hillslopes adjacent to the floodplain. Hay production and some logging have occurred on the floodplain over the last 100 years and a railroad traverses the western portion of the floodplain, but the river is wholly unregulated and generally lacks man-made structures (e.g., dikes and levees) that would influence patterns of floodwater inundation.

[8] The hydrology and geomorphology of the study site are well characterized [*Helton et al.*, 2012; *Poole et al.*, 2002, 2004, 2006]. The floodplain is constrained laterally by bedrock valley walls and bounded upstream and downstream by canyon segments with bedrock river beds. The annual flow regime of the fifth-order river is dominated by snowmelt, with a mean discharge of 80 m³ s⁻¹ and mean peak discharge of 600 m³ s⁻¹ (discounting the extraordinary peak discharge of nearly 4000 m³ s⁻¹ that occurred in 1964) [*Poole et al.*, 2004]. Annual spring floods inundate large areas of the non-channel floodplain surface [*Helton et al.*, 2012].

[9] Complex channel morphology and coarse, well-sorted sediments on the floodplain facilitate high rates of surface-subsurface water exchange with an extensive alluvial aquifer that is greater than 25 m thick near the upstream end of the floodplain and decreases to approximately 5 m thick near the downstream end of the floodplain. The aquifer spans the width of the floodplain (up to 1.5 km), and is constrained by an underlying aquiclude of clay deposits and bedrock [*Stanford et al.*, 1994].

[10] Within this study site, we consider the alluvial aquifer as an expansive hyporheic zone, because subsurface flow through the alluvium is recharged predominantly from the river channel [*Poole et al.*, 2006]. The main channel of the river loses approximately 30% of its base flow to the
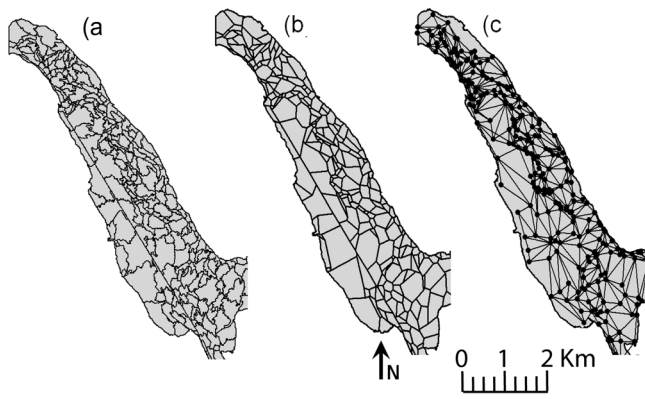
Figure 2. Plan view of model patches for the Nyack Floodplain (a) surface and (b) subsurface. (c) Example of link-and-node network created from subsurface patches in Figure 2b. (This figure has been adapted from an image in *Helton et al.* [2012], ©2012 Elsevier B.V. Reproduced by permission.)

underlying alluvial aquifer as it passes over the upstream 1/3 of the floodplain's length [*Stanford et al.*, 2005]. Water that recharges the alluvial aquifer flows down-valley in the subsurface, then later discharges back to the surface, either into the main channel or into spring channels. Spring channels subsequently flow along or across the floodplain until they rejoin a main river channel before the water flows off the floodplain, into the downstream canyon.

3. Model Description

[11] We linked empirical temperature and oxygen models with a mechanistic hydrogeomorphic model of the Nyack study site [*Helton et al.*, 2012]. Temperature and oxygen models were derived from comparisons between data sets of observed temperature and DO patterns with previous simulations of hydrologic residence time. We then integrated the empirical temperature and oxygen models into the existing hydrogeomorphic model of surface and subsurface water storage, flux, and exchange within the Nyack study site.

3.1. Hydrogeomorphic Model

[12] We used results from a hydrogeomorphic model applied by *Helton et al.* [2012] and originally developed by *Walton et al.* [1995] . The model is a finite volume, or "link and node," model in which the floodplain is divided into discrete patches, represented by nodes in a three-dimensional irregular lattice network (Figure 2). One-dimensional flows are calculated along links between adjacent nodes in all three spatial dimensions. Thus, the model represents (1) horizontal surface water flow and floodplain inundation, (2) horizontal and vertical subsurface flow, and (3) vertical exchange between surface and subsurface waters.

[13] The method used to delineate model patches was developed for low-relief landscapes and analyzes patterns of potential surface water connectivity across the floodplain to delineate patch boundaries [*Jones et al.*, 2008], based on a digital elevation model (DEM) derived from light detection and ranging (LiDAR) data (± 10 cm vertical accuracy, 1 m^2 grid cell size). The patch boundaries represent hydrologic divides, which are the most significant topographic obstacles

to surface water connectivity and inundation across the floodplain. A vertically stacked column of underlying subsurface patches was delineated for each surface patch (Figure 3). The subsurface layers include soil, 'shallow' alluvial aquifer, and 'deep' alluvial aquifer. Thicknesses of each layer within each patch were determined based on empirical relationships derived from well logs collected throughout the study site.

[14] *Helton et al.* [2012] performed a model simulation for the period from 1 November 1996 to 31 December 2000. Consecutively, these years encompassed one relatively high, one relatively low, and two intermediate snowmelt-driven hydrographs, thus representing the inter-annual range of hydrologic conditions expected at the study site.

3.2. Simulated Hydrologic Residence Time

[15] To parameterize the temperature and dissolved oxygen models (see below), we used estimates of hydrologic residence time from the river channel through the aquifer to each well where temperature and DO were measured. These estimates were derived from a particle tracking postprocessor, developed and implemented by *Helton et al.* [2012], that routes particles through the model domain (the link-and-node lattice representing the channel-floodplain-aquifer hydrosystem) based on model output. The particle tracker simulates the release of conservative tracer particles at a user-specified time and model node, assuming particles move along links at the same velocity as water. Thus, conservative tracer particle releases track the movement of water molecules through the study site, calculating the location of each particle within the modeled network over time. When a
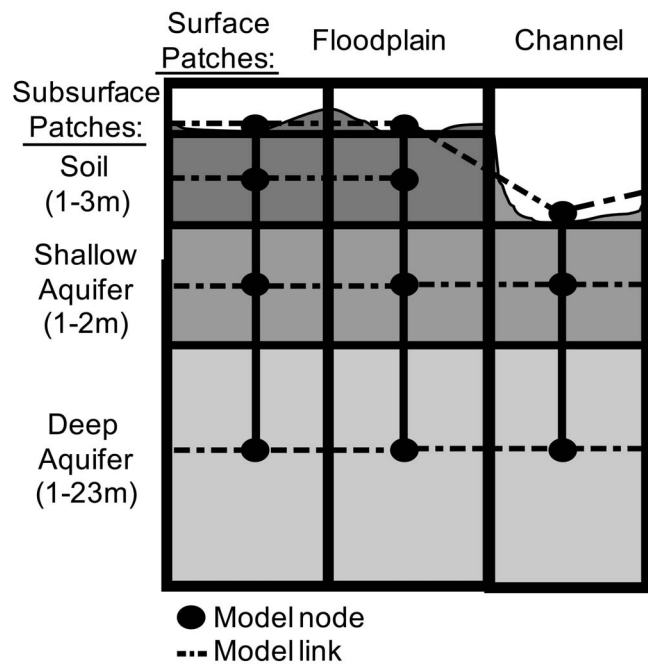

Figure 3. Cross-sectional view of model links and nodes. Links connect nodes both laterally and vertically among subsurface nodes and vertically between surface and subsurface nodes. Channel patches do not have underlying soil layers. (This figure has been adapted from an image in *Helton et al.* [2012], ©2012 Elsevier B.V. Reproduced by permission.)
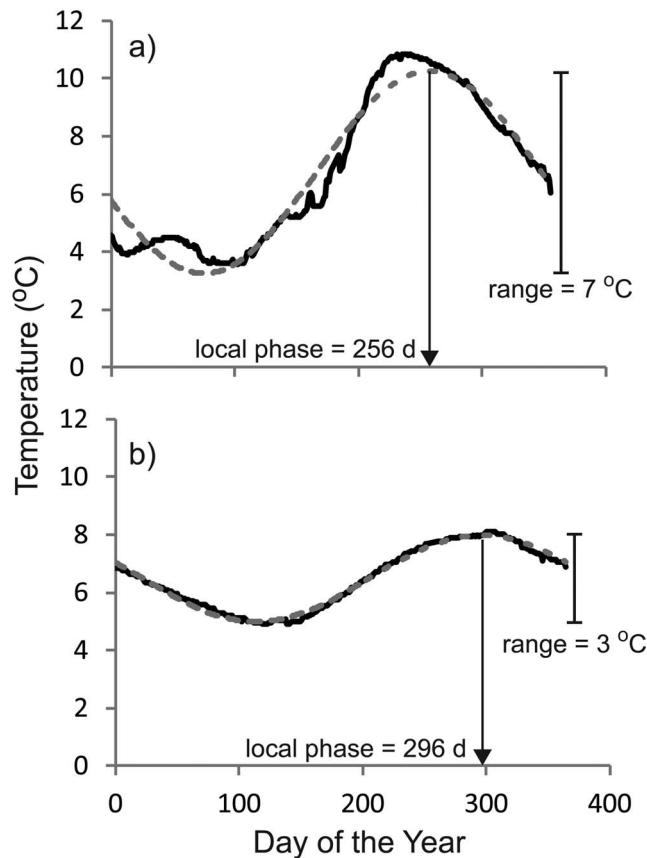
Figure 4. Examples of temperature range and local phase model fits (equation (1); see text) used in model parameterization. Black lines are observed data and gray dashed lines are model fits. Data are presented for observation wells with simulated mean hydrologic residence times of (a) 133 and (b) 261 days.

particle reaches a model node, the particle is routed along a random outflow link from the node, where the likelihood of entering each outflow link is proportional to the volume of water flowing through the outflow link.

[16] *Helton et al.* [2012] conducted nine simulated instantaneous particle releases within the model; three during base flow, three during rising limbs, and three during falling limbs of annual hydrographs. We calculated the travel time of each particle from its time of instantaneous release at the upstream end of the simulated floodplain to its arrival at each node. The average of these travel times for all the particles arriving at a given node was considered the mean hydrologic residence time of water arriving at that node. This mean residence time is an overall average of the hydrologic residence time distributions experienced by the nine parcels of simulated water labeled by the nine particle releases. The mean simulated residence times used for this analysis were the average over the entire simulation, and thus were constant for each model node across season and discharge conditions.

[17] This measure of hydrologic residence time is likely an overestimate of the actual residence time at any given location because particles are forced to travel along modeled links between model nodes, even where links are not perpendicular to isopleths of groundwater head. Thus, mean hydrologic

residence time is a measure of relative, not absolute, water residence time. However, our estimates of residence time span a similar range to prior simulations based on the MODFLOW groundwater model and MODPATH particle tracking software, which estimated groundwater flow paths with residence times up to 1.5 years [*Diehl*, 2004].

3.3. Temperature Model

[18] The relationship between simulated mean hydrologic residence time and observed temperature in corresponding wells was used to develop an empirical model that simulates spatial and temporal patterns of temperature across the study site. We obtained temperature records from 40 wells and surface water sites spanning the floodplain laterally, longitudinally, and vertically (Figure 1a). The data set consisted of 1) hourly temperature logger data for one to two years (data collected from 23 July 2002 to 22 November 2004 and from 3 July 2008 to 15 October 2009) for each of 12 wells and three surface water sites, 2) hourly temperature logger data for less than a year (2 to 11 months; data collected from 22 September 2002 to 16 July 2004) for each of 20 wells, and 3) manual monthly temperature measurements for 5 additional wells from 1 May 2008 to 15 October 2009. Data records exceeding one year were used for temperature model development (n = 20), and data records less than one year were used to evaluate the temperature model (n = 20).

[19] Monitoring wells consisted of two- or three-inch schedule 40 PVC slotted over the depth of the well, installed to depths of 5 to 8 m (see *Diehl* [2004] for well installation details). Wells were instrumented with either VEMCO™ Minilog data loggers or Solinst Levelloggers® to record hourly temperature. Loggers were installed at multiple depth intervals on smaller diameter PVC inserted into the wells, and baffles were attached to the PVC inserts between loggers to isolate well water at different depths. Manual temperature measurements were recorded with a YSI 85 (Yellow Springs Instruments, Inc.) in conjunction with DO measurements (see Section 3.4, below).

[20] We aggregated the hourly temperature records to daily means and analyzed the model development data according to *Arrigoni et al.* [2008]. Specifically, we fit a cosine wave to the observed annual cycle of temperature for each sampling location by minimizing the root mean squared error for the following equation [*Arrigoni et al.*, 2008] (Figure 4):

$$T_d = (0.5R)\cos[(d - P_L)c] + M, \qquad (1)$$

where T_d is the observed mean daily water temperature (°C) for a given day of the year (d), M is the mean annual temperature in °C, R is the annual temperature range (or wave amplitude) in °C, and P_L is the local phase (day of year when the peak temperature at the sampling location occurred) and c is $2\pi/365$, a constant to convert day of the year to radians, such that the calculated cosine wave has a period of one year. Since P_L is cyclical over a 365 day period, we constrained P_L to range between 1 and 365 when fitting parameters. The phase shift, or change in timing of peak temperature from the river to a given location within the aquifer, can be defined as the difference between the local phase at a given location (P_L) minus the annual temperature phase in the river (P). Note that temperature is not a
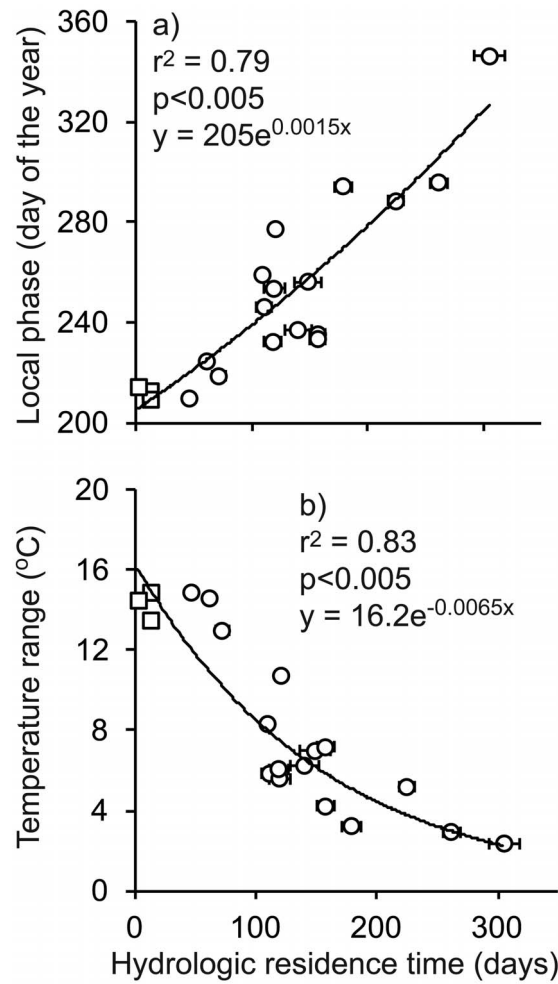
Figure 5. (a) Annual temperature local phase (day of the year that peak temperature occurs at a specific location, 1 January = 1 day), and (b) annual temperature range (°C) derived from surface and well water temperature records versus simulated hydrologic residence time (days ± 1 SE) at the location of the temperature logger.

conservative hydrologic tracer. The phase shift is positively related to hydrologic transport time, but a heat transport model that includes conduction with sediments would be necessary to provide a direct estimate of hydrologic transport time from temperature signals [*Anderson*, 2005].

[21] We used the relationships between the mean simulated residence time and characteristics of the corresponding observed annual temperature cycles (R and P_L) (Figure 5) to estimate average daily temperature for each model node for each day of the year. First, we used the mean simulated hydrologic residence time for each node to estimate R and P_L for that node based on empirical power law relationships (Figure 5). Then, we calculated the average daily temperatures for each node from its R and P_L (equation (1)), thus populating every node of the model with daily average temperature estimates during the period of simulation. Thus, we used an empirical extrapolation to estimate the spatial distribution of temperature for each day of the year across the study system.

3.4. Dissolved Oxygen Model

[22] The model uses a mass balance approach to simulate DO concentration for each node within the floodplain subsurface, based on advection to and from adjacent cells and microbial uptake:

$$DO_t = DO_{t-\Delta t} + \sum_{inflows} [DO]_{in,t} Q_{in,t} - \sum_{outflows} [DO]_{out,t} Q_{out,t} - u_{DO,t} \tag{2}$$

and

$$[DO]_t = \frac{DO_t}{V_t}, \tag{3}$$

where DO_t is the mass of dissolved oxygen at time t in a given model node, Δt is the time step of the model, $\left(\sum_{inflows} [DO]_{in,t} Q_{in,t} \right)$ is the sum of advective transport of DO into the model node (mg h^{-1}), $\left(\sum_{outflows} \left[[DO]_{out,t} Q_{out,t} \right] \right)$ is the sum of advective transport of DO out of the model node (mg h^{-1}), $u_{DO,t}$ is biological uptake, $[DO]_t$ is DO concentration (mg L^{-1}), and V_t is water stored within a given model node. The rate of water flux between nodes (Q ; L h^{-1}) and water storage within nodes (V_t; L) is derived from the hydrogeomorphic model, described above.

[23] For subsurface model nodes, DO uptake ($u_{DO,t}$) is simulated at a given time and DO concentration with a temperature-dependent Michaelis-Menten uptake function:

$$u_{DO,t} = \frac{u_{max}[\mathbf{DO}]}{K_s + [\mathbf{DO}]}, \tag{4}$$

where [DO] is concentration of dissolved oxygen (mg L^{-1}), u_{max} is the maximum uptake rate of DO (mg L^{-1} h^{-1}), and K_s is the half-saturation concentration of DO (mg L^{-1}). Maximum uptake was observed to be linearly related to water temperature, so a simple empirical relationship was used to simulate u_{max}:

$$u_{max} = aT + b, \tag{5}$$

where a and b are the slope and intercept of the linear regression of observed data and T is water temperature (°C).

[24] We parameterized and evaluated the DO model with a large (n = 850) data set of DO concentration measurements that spanned the Nyack study site longitudinally, laterally, and vertically (Figure 1b), and across seasonal variability and river discharge (Table 1). Data included measured DO concentration from 2003, 2004, 2008, and 2009 collected during 28 sampling events. Between 7 and 21 wells and 2 and 5 main stem surface water sites were sampled during each sampling event. Wells were typically sampled at two discrete depths: near the water table and at least 2 m below the water table, providing observed data corresponding to both our shallow and deep modeled aquifer layers.

[25] Wells were sampled using a modified straddle packer design to sample at discrete depth intervals. Immediately prior to collecting each DO measurement, wells were pumped with a hand-operated diaphragm pump until water ran clear for the entire depth of the well. We then inserted

Table 1. Simulated and Observed Dates for Dissolved Oxygen Model Evaluation[a]

Flow Comparison Type[b]	Simulated Dates	Observed Dates
Fall base	24–30 Oct 1998	15–16 Oct 2009
	21–22 Nov 1998	7–10 Nov 2003
	10–14 Sep 1999	10–11 Sep 2008
	23–25 Sep 1999	16–17 Sep 2009
	25–30 Sep 1999	26–30 Oct 2004
	25–30 Sep 1999	25 Sep–23 Oct 2008
Spring peak	19–22 May 1999	25–30 May 2004
	25–29 May 1999	28 May–1 Jun 2009
	14–15 Jun 1999	13–14 Jun 2008
	21–23 Jun 1999	26–27 Jun 2008
Spring rising	20–25 Apr 1999	20–21 Apr 2009
	20–25 Apr 1999	5–12 Apr 2004
	12–15 May 1999	1–2 May 2008
Summer base	23–29 Aug 1999	11–12 Aug 2008
	23 Aug–1 Sep 1999	17–20 Aug 2009
	28 Aug–1 Sep 1999	28 Aug 2008
Summer falling	14 Jun 1999	18 Jun 2009
	16 Jul 1999	1 Jul 2009
	17–19 Jul 1999	15–16 Jul 2008
	2–5 Jul 1999	2–8 Jul 2008
	25–26 Jul 1999	15–16 Jul 2009
	10–11 Aug 1999	30 Jul 2008
	13–20 Aug 1999	25 Jul–4 Aug 2004
Winter base	11–14 Jan 1999	14–15 Jan 2009
	2–4 Dec 1998	3–4 Dec 2008
	15–24 Feb 1999	18–23 Feb 2004
	20–21 Mar 1999	26–28 Mar 2009
	8–10 Mar 1999	4–14 Mar 2009

[a]For each range of simulated dates, average modeled DO concentration was calculated for each model node. These average concentrations were compared to measured DO concentrations from observed dates for model nodes that correspond spatially to sampled wells.

[b]Pairs of simulated and observed dates were grouped according to season (winter, summer, spring, and fall) and river discharge condition (base flow and peak, rising, and receding ("falling") flood flows).

tubing that was slotted at the bottom and baffled with foam packers to isolate one-meter intervals for a discrete depth sample into the well. A 12V electric submersible pump (Whale Submersible 881, Whale Systems Specialists) was then inserted into the tubing, and the isolated well segment was purged again until DO measurements in the pump effluent stabilized. Measurements were collected using a YSI 55 dissolved oxygen probe (Yellow Springs Instruments, Inc.) in 2003 and 2004 (data reported by *Reid* [2007]), and with a YSI 85 dissolved oxygen probe in 2008 and 2009.

[26] The monitoring data set was divided into parameterization data and evaluation data. Evaluation data included 820 DO concentration measurements taken across the floodplain and seasons. The parameterization data set (n = 30) was selected from one surface water and four well locations sampled on six dates. The wells were installed along a paleochannel, which is a preserved cobble-boulder bed of a historic river channel that fills over time with finer sediments creating preferential flow paths in the floodplain subsurface [*Poole et al.*, 1997]. Paleochannel features were identified with Ground Penetrating Radar at the well locations [*Hawkins*, 2003], and historical aerial photographs confirm that the Middle Fork of the Flathead River flowed through this section of the floodplain [*Whited et al.*, 2007].

[27] We fit DO uptake parameters for each of six sampling dates by finding the u_{max} and K_s parameters that minimized the root mean squared error between predicted DO

concentrations and observed DO concentrations from the parameterization data set (Figure 6). We estimated the hydrologic residence time corresponding to each well location based on output from the particle tracking model. Our simulated residence times are relative and not absolute residence times, so biological parameters developed here should not be extrapolated to other systems. We used the average K_s value across the six dates (4.5 mg L^{-1}) and the relationship between u_{max} and water temperature (Figure 7a) for floodplain-scale simulations. The model uses this observed relationship between u_{max} and temperature to simulate u_{max} within each model node over time (Figure 7b).

[28] The model requires DO concentrations in surface water as input. Therefore, for surface model nodes, we estimated DO concentrations based on the linear empirical relationship between point measurements of DO concentration and temperature taken in the main stem of the Middle Fork Flathead River at the study site (Figure 8).

4. Model Simulation and Evaluation

[29] We simulated daily DO and temperature dynamics for one year, which corresponded to the intermediate flow year from the previously run hydrologic simulations, 1 November 1998 to 31 October 1999. We ran the model for one simulation year prior to 1 November 1998 to assure that initial conditions were unlikely to affect model output.

[30] To verify the accuracy of our temperature model, we compared predicted daily average temperatures to daily average temperatures derived from 20 temperature records that spanned 2 to 11 months in 2002, 2003, 2004, 2008, and 2009 (see section 3.3 above for data description; well locations shown in Figure 1a). Since we did not have temperature records for the hydrologic simulation year, we compared observed values to predicted values on the same day of the year.

[31] We evaluated the DO model by comparing model output to observed data from 2003, 2004, 2008, and 2009 (see section 3.4 above for data description; well locations shown in Figure 1b). Since we did not have observed data for the simulation year, we compared simulated values to observed values collected in the same month of the year and with a similar river discharge (Table 1). River discharges for observed dates were within 5% of river discharge for simulated dates. We categorized each simulated versus observed comparison by season and river discharge condition (Table 1). Seasons included winter, summer, spring, and fall. Discharge conditions included base flow, peak flow, the rising limb of the flood spate before peak flow ("rising"), and the falling limb of the flood spate after peak flow ("falling").

5. Results

[32] Observed water temperature ranged from 0.5 to 16.0°C in surface waters and 0.1 to 15.5°C within the aquifer, varying longitudinally, laterally and vertically, and across different river discharge conditions and seasons. The temperature model fit the observed temperature data from 20 sampling locations well ($r^2_{1:1}$ = 0.66; RMSE = 1.27°C; Figure 9). The slope of the linear regression for simulated versus observed values was less than one (Figure 9), and model residuals (predicted minus observed temperature)
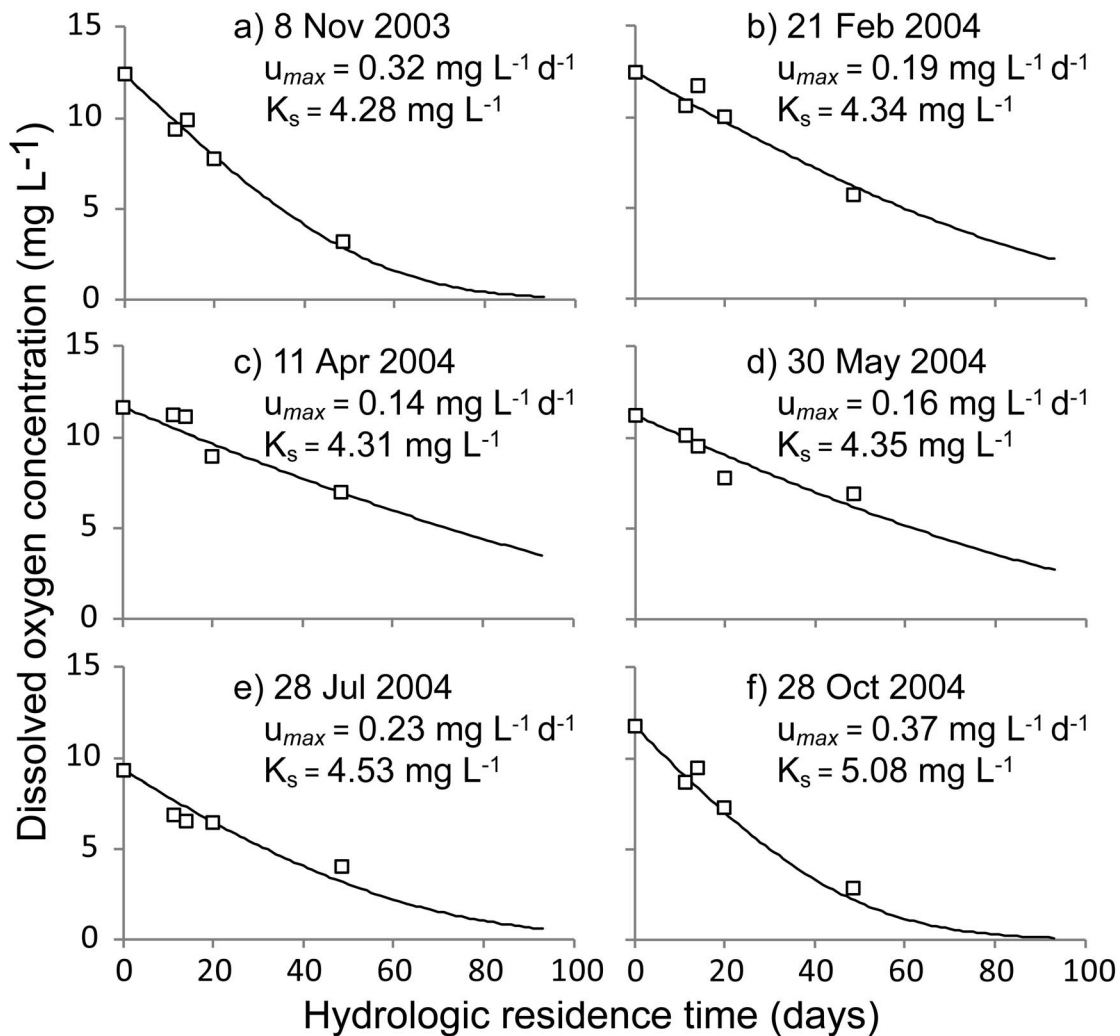
Figure 6. Observed (white squares) and parameterized model fit (black lines) of dissolved oxygen concentrations versus simulated hydrologic residence time for (a) 8 Nov 2003, (b) 21 Feb 2004, (c) 11 Apr 2004, (d) 30 May 2004, (e) 28 Jul 2004, and (f) 28 Oct 2004.

were negatively correlated to observed temperature (r^2 = 0.31; $p < 0.001$), suggesting the model modestly under-predicts temperature at high temperatures and over-predicts temperature at low temperatures.

[33] Observed DO concentration ranged from 8.44 to 13.1 mg L^{-1} in surface water and from 0.14 to 12.8 mg L^{-1} within the aquifer, varying longitudinally, laterally and vertically, and across different river discharge conditions and seasons. The DO model explained substantial variation in the whole data set ($r^2_{1:1}$ = 0.58; Figure 10) and among seasons (Table 2). The DO model fit varied across seasons and flow conditions, with model explained variance ($r^2_{1:1}$) ranging from 32% for spring peak flows to 71% for winter base flow conditions (Table 2 and Figure 11). Model residuals (predicted minus observed DO concentration) were unrelated to observed DO for the full data set ($p > 0.05$). Among seasons, model residuals were negatively correlated to observed DO during spring peak flow (r^2 = 0.31; $p < 0.001$), summer base (r^2 = 0.32; $p < 0.001$), and summer falling (r^2 = 0.24; $p < 0.001$). Residuals were unrelated to observed DO for fall and winter base flows and spring rising flows ($p > 0.05$). Simple

linear regressions between predicted and observed values always yielded a slope less than one, independent of season or discharge conditions (Table 2).

6. Discussion

6.1. Scaling Understanding of Flow Path Oxygen Dynamics

[34] The simple models of temperature and DO uptake integrated with the relatively complex three dimensional hydrogeomorphic model explained a substantial amount of variation in measured DO concentrations across the study site and through time (Figures 10 and 11 and Table 2). These results illustrate the importance of understanding the hydrogeomorphic dynamics of a river to simulate spatio-temporal patterns of ecosystem processes. The relationship between simulated and observed DO was strong across among seasons and river discharge conditions (Figure 11), indicating that the drivers of oxygen dynamics simulated by the model (advection, uptake, and temperature) are generally
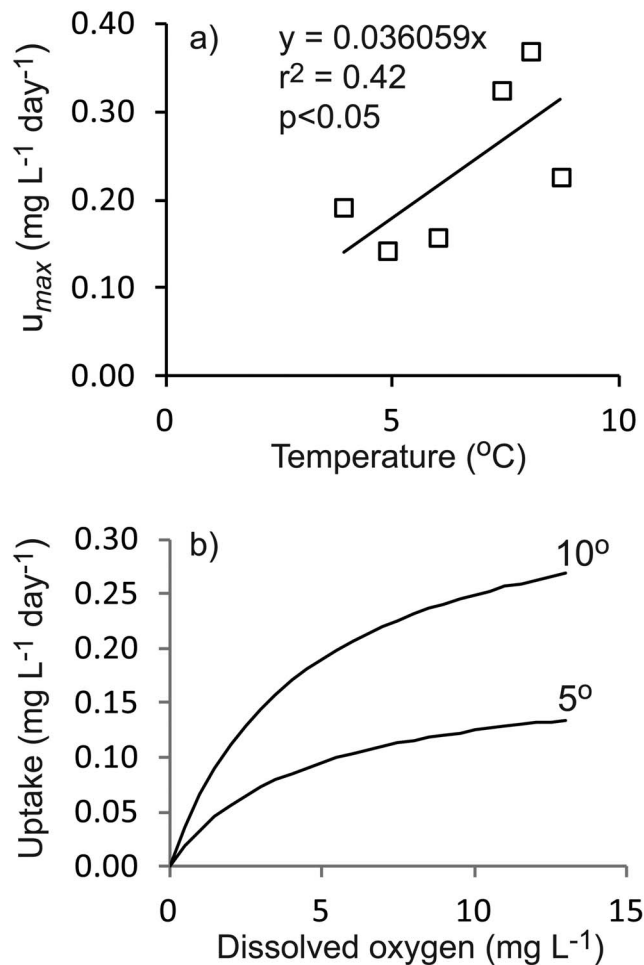
Figure 7. (a) Maximum uptake rate for dissolved oxygen versus observed mean temperature for the six sampling dates shown in Figure 5. (b) Model relationship between oxygen uptake and concentration at 5 and 10°C.

paths of only a few meters. Scaling this observed pattern to DO dynamics along multiple, interactive flow paths (that can be hundreds of meters long) requires quantifying hydrologic advection of DO across time and space, as we have attempted to do here. The results of our effort show the potential to scale understanding of short flow path scale dynamics across much larger, complex, three-dimensional river-floodplain-aquifer systems with relatively simple biogeochemical models, when hydrologic advection is adequately represented.

6.2. Simulating Temperature Dynamics

[37] Previous research shows that heat (as measured by temperature) can be used as a groundwater tracer [reviewed by *Anderson*, 2005] and that temperature range decreases and phase shift (or difference in surface and subsurface peak temperatures) increases with subsurface flow path length in extensive hyporheic zones [*Poole et al.*, 2008]. A strong correlation between the annual temperature cycle and mean simulated hydrologic residence times (Figure 5) indicates that our simulated hydrologic residence time is an accurate representation of the relative hydrologic residence times within the Nyack study site. The relationship between annual temperature cycles (local phase and range) and simulated hydrologic residence times correspond qualitatively to patterns observed by *Arrigoni et al.* [2008] for diel temperature cycles: as hydrologic residence time increases, the range of water temperature decreases (the temperature signal is "buffered") and the local phase, or day of year to peak temperature at a given location, is delayed (the temperature signal is "lagged") relative to surface water.

[38] The strong relationship between characteristics of the temperature signal and simulated hydrologic residence times allowed us to reasonably extrapolate average daily temperature dynamics across the Nyack study site (Figure 9). Although the empirical model explained substantial variation in the observed data set, the model tended to over-predict temperatures at low temperatures and under-predict temperatures at high temperatures. Relatively shallow aquifers can be affected by surface temperatures [*Taniguchi*,
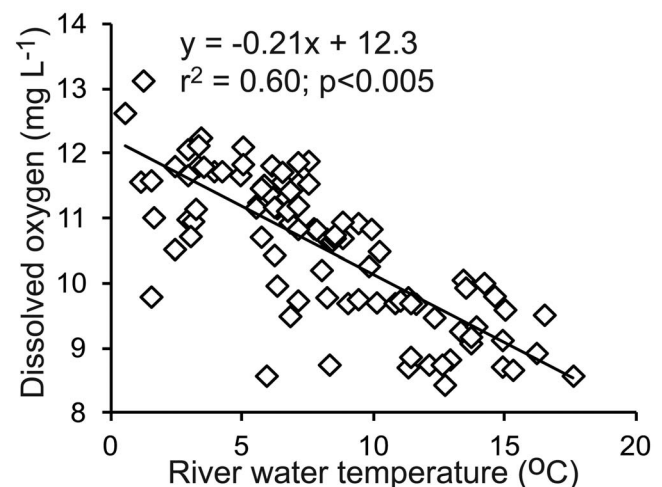
applicable across a wide array of conditions that vary with space and time within the Nyack Floodplain aquifer.

[35] The slope of the relationship between simulated and observed DO concentrations was always less than one, and the model typically under-predicted DO concentrations (Figure 11 and Table 2). This suggests that the model over-predicts DO uptake, or that there is some additional source of DO along subsurface flow paths. The model may over-predict DO uptake because of limitation by carbon or other nutrients to microbial respiration [e.g., *Zarnetske et al.*, 2011]. The model also does not account for some potential sources of DO, including exchange between saturated sediments and overlying unsaturated sediments or the atmosphere [*Smith et al.*, 2011], and DO inputs from plant roots to the subsurface [*Colmer*, 2003; *Reddy et al.*, 1989]. Recent research by *Smith et al.* [2011] suggests that diffusion may be an important DO source for some areas in the Nyack aquifer.

[36] Observations of declines in DO along one-dimensional hyporheic flow paths are common [*Findlay et al.*, 1993, 2003; *Fernald et al.*, 2006; *Holmes et al.*, 1994], but these studies typically occur in small streams and along flow

Figure 8. Observed dissolved oxygen concentration versus river water temperature for the Middle Fork Flathead River measured from surface water on dates listed in Table 1.
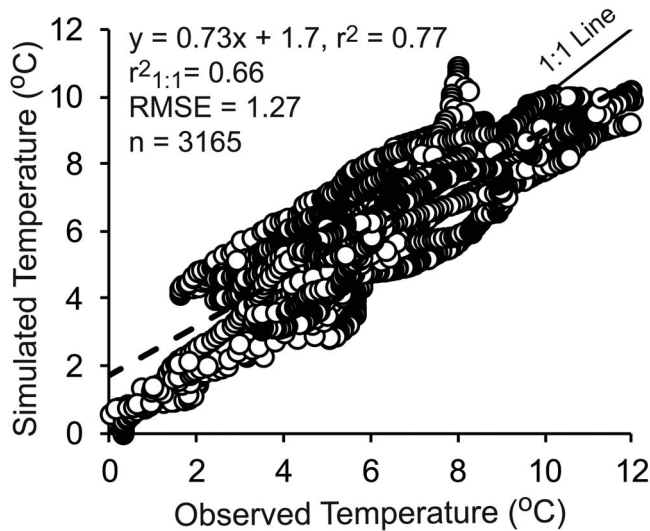
Figure 9. Simulated versus observed daily average temperature from wells with 2–11 month temperature records across the floodplain (Figure 1a, circles). Dashed line shows the simple linear regression fit, and solid line the 1:1 line.

1993; *Vogt et al.*, 2012], so Nyack subsurface water may experience additional warming during summer months and cooling during winter months. Alternatively, and perhaps more likely considering the large volume of the aquifer and high rates of flow through the aquifer [*Helton et al.*, 2012], the model represents the annual cycle of daily mean temperature as a cosine wave, a somewhat inaccurate simplifying assumption (e.g., Figure 4a) that may yield modest errors especially at peak and trough annual temperatures. In fact, one reason that this approach works well within the Nyack study site is the high hydrologic connectivity between nodes and the dominance of advective processes. Thus, a model like this might not be expected to work as well in systems where hydraulic conductivity is lower and a more mechanistic approach that accounts for non-advective influences of heat transfer would be necessary.

6.3. Spatial and Temporal Patterns in Fluvial Landscapes

[39] Hydrologically driven transport of solutes is fundamental for understanding and predicting important times and locations of biogeochemical processes (e.g., "hot moments
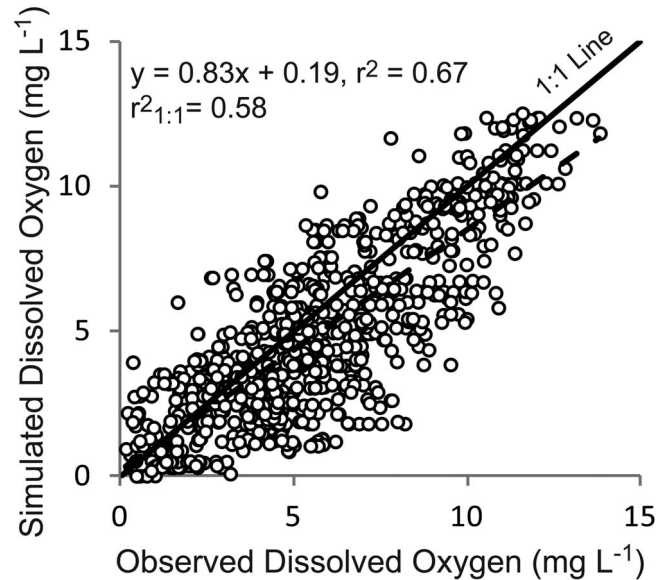

Figure 10. Simulated versus observed dissolved oxygen concentration from wells across the floodplain (Figure 1b) and among all seasons and discharge conditions (Table 1). Dashed line shows the simple linear regression fit, and solid line shows the 1:1 line. Additional model statistics are reported in Table 2.

and hot spots" [sensu *McClain et al.*, 2003]) that may drive whole-system rates of ecosystem processes. Ecohydrologic models for terrestrial hillslopes simulate hydrologically explicit biogeochemical dynamics, even predicting important times and locations of biogeochemical processes within hillslopes [*Band et al.*, 2001]. Our modeling framework for river-floodplain-aquifer systems is analogous to ecohydrologic models for terrestrial systems (reviewed by *Boyer et al.* [2006]; *Kulkarni et al.* [2008]). Our model results illustrate spatial and temporal patterns of temperature and oxygen dynamics within the alluvial aquifer of the Nyack Floodplain (Figure 12).

[40] Patterns of temperature (Figure 12, left) produced by the model illustrate the heterogeneity within the alluvial aquifer that results from complex multidimensional hydrologic dynamics. During wintertime (e.g., January, Figure 12), temperature tends to increase with distance from the river channel because river surface water (and hence near-channel

Table 2. Simulated Versus Observed Statistics for Dissolved Oxygen Model[a]

Data Set	n	[DO] (mg L^{-1})	$r^2_{1:1}$	RMSE (mg L^{-1})	NRMSE	SLR
Full data set	820	5.6 ± 3.0	0.58	1.95	0.14	$y = 0.83x + 0.19$; $r^2 = 0.67$
Winter base	107	7.2 ± 3.3	0.71	1.81	0.14	$y = 0.88x + 1.05$; $r^2 = 0.73$
Spring rising	83	7.2 ± 2.6	0.63	1.66	0.17	$y = 0.87x + 0.71$; $r^2 = 0.66$
Spring peak	115	6.0 ± 2.6	0.32	1.79	0.16	$y = 0.65x + 1.54$; $r^2 = 0.58$
Summer falling	187	5.3 ± 2.6	0.40	1.78	0.15	$y = 0.72x + 0.51$; $r^2 = 0.67$
Summer base	85	4.5 ± 2.5	0.38	2.03	0.22	$y = 0.62x + 0.54$; $r^2 = 0.57$
Fall base	242	4.7 ± 3.0	0.37	2.24	0.18	$y = 0.74x + 0.09$; $r^2 = 0.61$

[a]Abbreviations are as follows: n, number of observations; [DO], average observed DO concentration ±Std. Dev.; $r^2_{1:1}$, coefficient of determination calculated for 1:1 model lines (shown in Figures 10 and 11); RMSE, root mean square error; NRMSE, normalized root mean square error ($NRMSE = \frac{RMSE}{X_{obs,max} - X_{obs,min}}$, where $X_{obs,max}$ and $X_{obs,min}$ are the maximum and minimum observed DO concentrations, respectively); and SLR, simple linear regression. Last column shows simple linear regression equations and r^2 for simulated versus observed values. All SLRs were significant at $p < 0.001$. See Table 1 for a description of model comparison data sets.
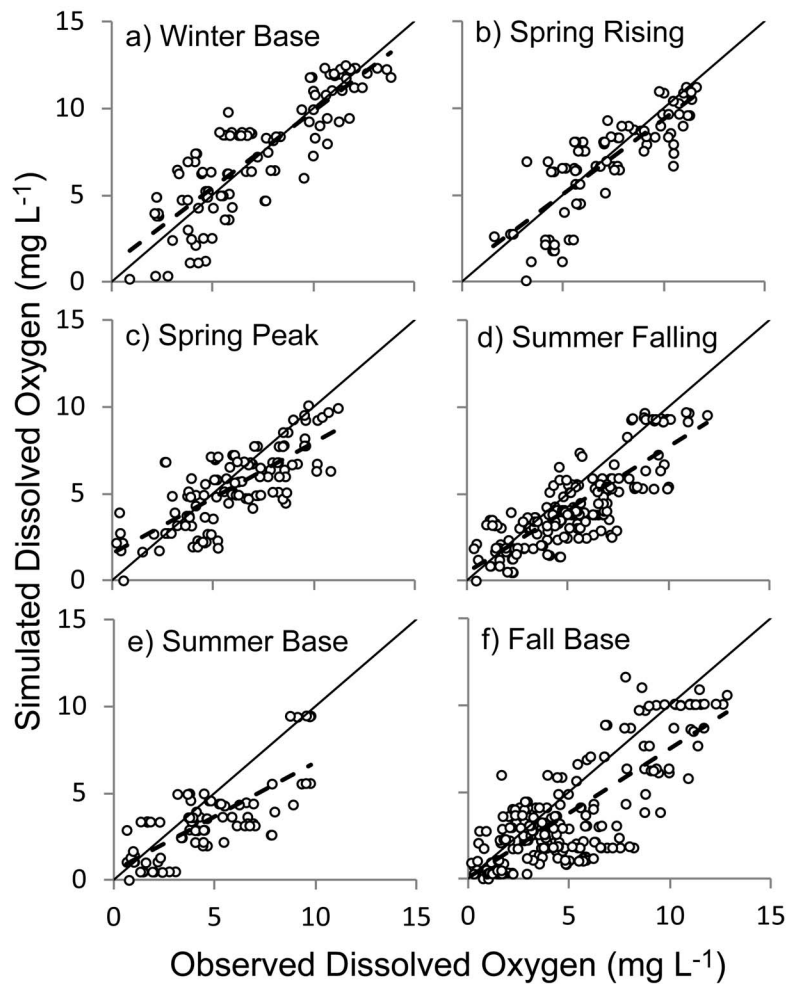
Figure 11. Simulated versus observed dissolved oxygen concentration across seasonal variability and discharge conditions: (a) winter base flow, (b) spring rising limb, (c) spring peak flow, (d) summer falling limb, (e) summer base flow, and (f) fall base flow. Dashed lines show the simple linear regression fits, and solid lines show the 1:1 lines. Model statistics are reported in Table 2.

aquifer water recently recharged from the river) is cooler than aquifer water farther from the channel that was recharged during warmer spring and summer months. The inverse of this pattern occurs during summer months (e.g., July, Figure 12), when river surface water is warmer than aquifer water that was recharged during colder fall and winter months. Spring and autumn (e.g., April and October, Figure 12) show less dramatic spatial patterns in temperature, since river water recharging the aquifer is similar in temperature to aquifer water. Thus, seasonal patterns alternate spatially between steep increases and decreases in, and relatively homogenous cool and warm aquifer temperatures.

[41] Spatiotemporal trends in simulated DO concentrations illustrate the influence of hydrologic dynamics on biogeochemical patterns (Figure 12, right). Dissolved oxygen concentrations within the alluvial aquifer range from near saturation to near zero during all seasons. Because DO concentrations decrease with residence time (as DO is taken up by biota), near channel DO is typically higher than DO concentrations farther from the channel. The steepest gradients of DO concentrations occur in the winter (e.g., January, Figure 12), when the river channel water recharging the aquifer is coldest relative to the warmer aquifer water. As river channel water temperature increases through the spring and summer, DO concentrations become more homogenous within the aquifer (e.g., changes in DO spatial gradient from January to July, Figure 12). During warmer months, higher temperatures cause lower saturated DO concentrations in water entering the aquifer and higher rates of biological uptake, hence lower near channel DO concentration within the aquifer and more homogenous patterns of DO across the aquifer (July, Figure 12). Thus, seasonal patterns shift spatially from steep spatial DO gradients that set up during the winter to shallower DO gradients, with overall lower DO concentrations, as the summer progresses.

[42] Although winter and summer months show general spatial trends from near-channel to the floodplain fringes, high variability in temperature and DO concentrations exists within the near channel alluvial aquifer. Localized areas of low DO concentrations, or high temperature relative to river water temperature in the winter (January, Figure 12) and low temperature relative to river water temperature in the summer (July, Figure 12), correspond to areas of upwelling, or aquifer discharge to the river channel. Alternating spatial
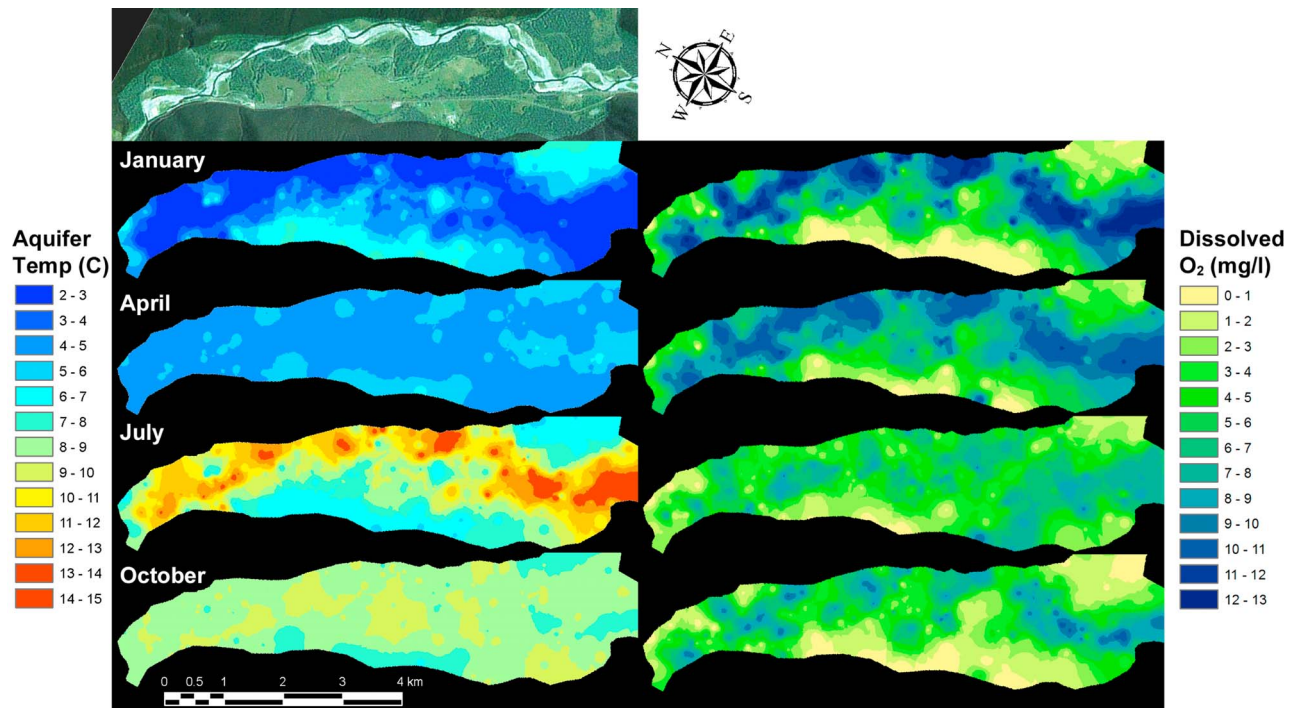
Figure 12. (top) Aerial photo of the Nyack Floodplain and (left) color maps of modeled temperatures and (right) dissolved oxygen concentrations within the shallow modeled layer of the alluvial aquifer across seasons. River flows north.

patterns of recently recharged ("new") aquifer water and discharging ("old") aquifer water create a spatial mosaic of temperature and dissolved oxygen that is more complex near the river channel.

[43] Model simulation results show how complex hydrologic dynamics create a shifting habitat mosaic [sensu *Stanford et al.*, 2005] of temperature and dissolved oxygen within the alluvial aquifer that likely influences a wide array of aquatic organisms and ecosystem processes [*Malard and Hervant*, 1999]. We can use the simulation model results to understand or develop hypotheses and predictions about spatial and temporal patterns of various ecological and biogeochemical phenomena.

[44] Localized areas of cool aquifer water discharging to the river channel during summer months creates important spawning and rearing habitats for cold-water fishes [e.g., *Eberle and Stanford*, 2010] and invertebrates [*Anderson*, 2008]. At the Nyack Floodplain, spatial patterns within the aquifer apparently influence local abundances of the many aquatic invertebrates that occur within the aquifer. Benthic species reside mostly within a few meters below and lateral to the river channel, but a wide variety of insects (mostly Plecoptera) and crustaceans occupy the entire aquifer, with insect larvae migrating from the aquifer to the channel to emerge as flying adults [*Stanford et al.*, 1994, 2005]. Abundances per species are consistently lower in areas of the aquifer where DO concentrations approach hypoxia [*Reid*, 2007]. Thus, the model may inform research that seeks to answer questions about the influence of environmental conditions on aquatic biota or to better understand the distribution and abundance of benthic species.

[45] Microbially mediated ecosystem processes occurring within the aquifer may also be linked to spatiotemporal patterns of temperature and dissolved oxygen. Microbial respiration drives declines in DO along subsurface flow paths [e.g., *Hedin et al.*, 1998]. Various aerobic and anaerobic microbial processes are likely correlated with patterns of dissolved oxygen. Low areas of DO concentrations may indicate important times and locations for denitrification, methanogenesis, or other anaerobic processes, whereas near channel areas of high DO concentrations may indicate high rates of aerobic processes, like nitrification.

[46] Because of highly variable DO concentrations near the channel (Figure 12), complex biogeochemical patterns may emerge as different suites of solutes are brought into contact with one another. For example, when flow paths of varying residence times converge (e.g., near channel localized areas of discharging aquifer water with low DO intersect recharging aquifer water with high DO), "hot spots and moments" of aerobic processes that use anaerobic end products may occur, such as the consumption of methane by methane oxidizing microbes. Thus, simulated spatiotemporal patterns of temperature and dissolved oxygen provide predictions about when and where biogeochemical processes are likely to occur within the aquifer, which provide a tool for linking point measurements of these processes to their overall influence across multidimensional fluvial landscapes.

7. Conclusions

[47] The coupled hydrogeomorphic-temperature-dissolved oxygen simulation model explained substantial variance in temperature and DO observations made across seasonal

variability in discharge for the alluvial aquifer of the Nyack Floodplain. Our results illustrate how one-dimensional flow path biogeochemical dynamics can be reasonably scaled to a larger three-dimensional river-floodplain system by integrating a simple biogeochemical model with a detailed floodplain temperature and hydrogeomorphic model. This research provides an approach for scaling spatially and temporally dynamic biogeochemical processes from flow paths to fluvial landscapes, particularly large gravel bedded river systems. It shows that spatiotemporal complexity in biogeochemical patterns, including "hotspots and hot moments," may emerge from relatively simple biogeochemical dynamics operating within a complex, three-dimensional hydrologic system, and thus highlights the importance of understanding the hydrogeomorphic template of a system that drives the hydrologic flux and storage of biogeochemical constituents. These coupled models provide the first step toward a mechanistic prediction of the times and locations that may have disproportionate influence on biogeochemical processes within expansive three dimensional fluvial landscapes.

References

Anderson, M. L. (2008), The edge effect: Lateral habitat ecology of an alluvial river floodplain, PhD diss., Univ. of Montana, Missoula.

Anderson, M. P. (2005), Heat as a ground water tracer, *Ground Water*, *43*, 951–968, doi:10.1111/j.1745-6584.2005.00052.x.

Arrigoni, A. S., G. C. Poole, L. A. K. Mertes, S. J. O'Daniel, W. W. Woessner, and S. A. Thomas (2008), Buffered, lagged, or cooled? Disentangling hyporheic influences on temperature cycles in stream channels, *Water Resour. Res.*, *44*, W09418, doi:10.1029/2007WR006480.

Baker, M. A., H. M. Valett, and C. N. Dahm (2000), Organic carbon supply and metabolism in a shallow groundwater ecosystem, *Ecology*, *81*, 3133–3148, doi:10.1890/0012-9658(2000)081[3133:OCSAMI]2.0.CO;2.

Band, L. E., C. L. Tague, P. Groffman, and K. Belt (2001), Forest ecosystem processes at the watershed scale: Hydrological and ecological controls of nitrogen export, *Hydrol. Processes*, *15*, 2013–2028, doi:10.1002/hyp.253.

Bencala, K. E., M. N. Gooseff, and B. A. Kimball (2011), Rethinking hyporheic flow and transient storage to advance understanding of stream-catchment connections, *Water Resour. Res.*, *47*, W00H03, doi:10.1029/2010WR010066.

Boyer, E. W., R. B. Alexander, W. J. Parton, C. S. Li, K. Butterbach-Bahl, S. D. Donner, R. W. Skaggs, and S. J. Del Gross (2006), Modeling denitrification in terrestrial and aquatic ecosystems at regional scales, *Ecol. Appl.*, *16*, 2123–2142, doi:10.1890/1051-0761(2006)016[2123:MDITAA]2.0.CO;2.

Colmer, T. D. (2003), Long-distance transport of gases in plants: A perspective on internal aeration and radial oxygen loss from roots, *Plant Cell Environ.*, *26*, 17–36, doi:10.1046/j.1365-3040.2003.00846.x.

Dahm, C. N., N. B. Grimm, P. Marmonier, H. M. Valett, and P. Vervier (1998), Nutrient dynamics at the interface between surface waters and groundwaters, *Freshwater Biol.*, *40*, 427–451, doi:10.1046/j.1365-2427.1998.00367.x.

Dent, C. L., N. B. Grimm, and S. G. Fisher (2001), Multiscale effects of surface-subsurface exchange on stream water nutrient concentrations, *J. N. Am. Benthol. Soc.*, *20*, 162–181, doi:10.2307/1468313.

Diehl, J. C. (2004), Hydrogeological characteristics and groundwater/river exchange in a gravel-dominated floodplain, Middle Fork of the Flathead River, northwestern Montana, MA thesis, Univ. of Montana, Missoula.

Eberle, L. C., and J. A. Stanford (2010), Importance and seasonal availability of terrestrial invertebrates as prey for juvenile salmonids in floodplain spring brooks of the Kol River (Kamchatka, Russian Federation), *River Res. Appl.*, *26*, 682–694.

Fellows, C. S., H. M. Valett, and C. N. Dahm (2001), Whole-stream metabolism in two montane streams: Contribution of the hyporheic zone, *Limnol. Oceanogr.*, *46*, 523–531, doi:10.4319/lo.2001.46.3.0523.

Fernald, A. G., D. H. Landers, and P. J. Wigington (2006), Water quality changes in hyporheic flow paths between a large gravel bed river and off-channel alcoves in Oregon, USA, *River Res. Appl.*, *22*, 1111–1124, doi:10.1002/rra.961.

Findlay, S., D. Strayer, C. Goumbala, and K. Gould (1993), Metabolism of streamwater dissolved organic carbon in the shallow hyporheic zone, *Limnol. Oceanogr.*, *38*(7), 1493–1499, doi:10.4319/lo.1993.38.7.1493.

Findlay, S., R. L. Sinsabaugh, W. V. Sobczak, and M. Hoostal (2003), Metabolic and structural response of hyporheic microbial communities to variations in supply of dissolved organic matter, *Limnol. Oceanogr.*, *48*(4), 1608–1617, doi:10.4319/lo.2003.48.4.1608.

Fisher, S. G., N. B. Grimm, E. Marti, R. M. Holmes, and J. B. Jones (1998), Material spiraling in stream corridors: A telescoping ecosystem model, *Ecosystems (N. Y.)*, *1*, 19–34, doi:10.1007/s100219900003.

Fisher, S. G., R. A. Sponseller, and J. B. Heffernan (2004), Horizons in stream biogeochemistry: Flowpaths to progress, *Ecology*, *85*, 2369–2379, doi:10.1890/03-0244.

Hawkins, C. R. (2003), Imaging the shallow subsurface using ground penetrating radar at the Nyack floodplain, Montana, MA thesis, Univ. of Montana, Missoula.

Hedin, L. O., J. C. von Fischer, N. E. Ostrom, B. P. Kennedy, M. G. Brown, and G. P. Robertson (1998), Thermodynamic constraints on nitrogen transformations and other biogeochemical processes at soil-stream interfaces, *Ecology*, *79*, 684–703.

Helton, A. M., G. C. Poole, R. A. Payn, C. Izurieta, and J. A. Stanford (2012), Relative influences of the river channel, floodplain surface, and alluvial aquifer on simulated hydrologic residence time in a montane river floodplain, *Geomorphology*, doi:10.1016/j.geomorph.2012.01.004, in press.

Holmes, R. M., S. G. Fisher, and N. B. Grimm (1994), Parafluvial nitrogen dynamics in a desert stream ecosystem, *J. N. Am. Benthol. Soc.*, *13*(4), 468–478, doi:10.2307/1467844.

Jones, K. L., G. C. Poole, S. J. O'Daniel, L. A. K. Mertes, and J. A. Stanford (2008), Surface hydrology of low-relief landscapes: Assessing surface water flow impedance using LIDAR-derived digital elevation models, *Remote Sens. Environ.*, *112*, 4148–4158, doi:10.1016/j.rse.2008.01.024.

Kulkarni, M. V., P. M. Groffman, and J. B. Yavitt (2008), Solving the global nitrogen problem: It's a gas! *Front. Ecol. Environ*, *6*, 199–206, doi:10.1890/060163.

Malard, F., and F. Hervant (1999), Oxygen supply and the adaptations of animals in groundwater, *Freshwater Biol.*, *41*, 1–30, doi:10.1046/j.1365-2427.1999.00379.x.

McClain, M. E., et al. (2003), Biogeochemical hot spots and hot moments at the interface of terrestrial and aquatic ecosystems, *Ecosystems (N. Y.)*, *6*, 301–312, doi:10.1007/s10021-003-0161-9.

McDonald, M. G., and A. W. Harbaugh (2003), The history of MODFLOW, *Ground Water*, *41*, 280–283, doi:10.1111/j.1745-6584.2003.tb02591.x.

Poole, G. C., R. J. Naiman, J. Pastor, and J. A. Stanford (1997), Uses and limitations of ground penetrating RADAR in two riparian systems, in *Groundwater/Surface Water Ecotones: Biological and Hydrological Interactions and Management Options*, *Int. Hydrol. Ser.*, edited by J. Gibert, J. Mathieu, and F. Fournier, pp. 140–148, Cambridge Univ. Press, Cambridge, UK, doi:10.1017/CBO9780511753381.019.

Poole, G. C., J. A. Stanford, C. A. Frissell, and S. W. Running (2002), Three-dimensional mapping of geomorphic controls on flood-plain hydrology and connectivity from aerial photos, *Geomorphology*, *48*(4), 329–347, doi:10.1016/S0169-555X(02)00078-8.

Poole, G. C., J. A. Stanford, S. W. Running, C. A. Frissell, W. W. Woessner, and B. K. Ellis (2004), A patch hierarchy approach to modeling surface and subsurface hydrology in complex flood-plain environments, *Earth Surf. Processes Landforms*, *29*, 1259–1274, doi:10.1002/esp.1091.

Poole, G. C., J. A. Stanford, S. W. Running, and C. A. Frissell (2006), Multiscale geomorphic drivers of groundwater flow paths: Subsurface hydrologic dynamics and hyporheic habitat diversity, *J. N. Am. Benthol. Soc.*, *25*, 288–303, doi:10.1899/0887-3593(2006)25[288:MGDOGF]2.0.CO;2.

Poole, G. C., S. J. O'Daniel, K. L. Jones, W. W. Woessner, E. S. Bernhardt, A. M. Helton, J. A. Stanford, B. R. Boer, and T. J. Beechie (2008), Hydrologic spiralling: The role of multiple interactive flow paths in stream ecosystems, *River Res. Appl.*, *24*, 1018–1031, doi:10.1002/rra.1099.

Reddy, K. R., W. H. Patrick Jr., and C. W. Lindau (1989), Nitrification-denitrification at the plant root-sediment interface in wetlands, *Limnol. Oceanogr.*, *34*, 1004–1013, doi:10.4319/lo.1989.34.6.1004.

Reid, B. L. (2007), Energy flow in a floodplain aquifer ecosystem, PhD diss., Univ. of Montana, Missoula.

Smith, M. G., S. R. Parker, C. H. Gammons, S. R. Poulson, and F. R. Hauer (2011), Tracing dissolved O_2 and dissolved inorganic carbon stable isotope dynamics in the Nyack aquifer: Middle Fork Flathead River, Montana, USA, *Geochim. Cosmochim. Acta*, *75*, 5971–5986, doi:10.1016/j.gca.2011.07.033.

Stanford, J. A., and J. V. Ward (1993), An ecosystem perspective of alluvial rivers: Connectivity and the hyporheic corridor, *J. N. Am. Benthol. Soc.*, *12*, 48–60, doi:10.2307/1467685.

Stanford, J. A., J. V. Ward, and B. K. Ellis (1994), Ecology of the alluvial aquifers of the Flathead River, Montana, in *Groundwater Ecology*, edited by J. Gilbert, D. L. Danielopol, and J. A. Stanford, pp. 367–390, Academic, San Diego, Calif.

Stanford, J. A., M. S. Lorang, F. R. Hauer (2005), The shifting habitat mosaic of river ecosystems, *Verh. Int. Ver. Theor. Angew. Limnol.*, *29*, 123–136.

Taniguchi, M. (1993), Evaluation of vertical groundwater fluxes and thermal properties of aquifers based on transient temperature-depth profiles, *Water Resour. Res.*, *29*(7), 2021–2026, doi:10.1029/93WR00541.

Vidon, P., and A. R. Hill (2004), Denitrification and patterns of electron donors and acceptors in eight riparian zones with contrasting hydrogeology, *Biogeochemistry*, *71*, 259–283, doi:10.1007/s10533-004-9684-1.

Vogt, T., M. Schirmer, and O. A. Cirpka (2012), Investigating riparian groundwater flow close to a losing river using diurnal temperature oscillations at high vertical resolution, *Hydrol. Earth Syst. Sci.*, *16*, 473–487, doi:10.5194/hess-16-473-2012.

Walton, R., T. H. Martin Jr., R. S. Chapman, and J. E. Davis (1995), Investigation of wetlands hydraulic and hydrological processes, model development, and application, *Tech. Rep. WRP-CP-6*, U.S. Army Corps of Eng., Waterways Exper. Stn., Vicksburg, Miss.

Whited, D. C., M. S. Lorang, M. J. Harner, F. R. Hauer, J. S. Kimball, and J. A. Stanford (2007), Climate, hydrologic disturbance, and succession: Drivers of floodplain pattern, *Ecology*, *88*, 940–953, doi:10.1890/05-1149.

Zarnetske, J. P., R. Haggerty, S. M. Wondzell, and M. A. Baker (2011), Dynamics of nitrate production and removal as a function of residence time in the hyporheic zone, *J. Geophys. Res.*, *116*, G01025, doi:10.1029/2010JG001356.